J. KOSAE Vol. 19, No. E4 (2003) pp. 149~155
Journal of Korean Society for Atmospheric Environment

Estimation of Total Precipitable Water in East Asia Using the MODIS Satellite Data

Seon Ki Park
Department of Environmental Science and Engineering, Ewha Womans University, Seoul, 120-750, Korea

(Received 22 August 2003, accepted 12 December 2002)

Abstract

In this study, the amounts of the total precipitable water (TPW) in both global and regional scale are estimated from the MODIS instrument, which is on-board the EOS satellites, Terra and Aqua. The estimation is made from the five near-infrared spectral bands, using a technique employing ratios of water-vapor absorbing channels centered at 0.905, 0.936, 0.940 μm with atmospheric window channels at 0.865 and 1.240 μm.

Through analyses of monthly and eight-days mean TPW, one can monitor characteristics of seasonal variations as well as amount and distribution (i.e., water resources) of TPW at both global and local regions. Long-term monitoring of TPW is essential to understand the regional variations of water resources in East Asia.

Key words : Water vapor, Total precipitable water, MODIS, Near-infrared bands

1. INTRODUCTION

There exist 24 key elements that are essential for the Earth environmental system and that can be measurable through the satellites of the Earth Observing Systems (EOS) program (NASA, 2003a), as noted by Barron *et al.* (1999). Among them, water vapor (WV) is one of the major elements that links all subcomponents of the Earth environmental system-atmosphere, land, ocean, and cryosphere. It is also a key element in hydrological cycle and climate of the Earth. WV plays a driving role in atmospheric circulation through energy transfer related to phase changes. The vertically integrated WV or total precipitable water (TPW) has a variety of applications, especially in forecasts of weather, hydrology and climate via a newly-emerged techniques of data assimilation. Especially monitoring seasonal and annual variations in TPW is important to monitor drought and desertification processes on regional scales.

Traditionally the WV profiles were retrieved from infrared (IR) sounders as a byproduct of retrieving the atmospheric temperature profiles, using a split window technique (e.g., Kleespies and McMillin, 1990; Chesters *et al.*, 1983). The derived WV profile, however, depends partly on the initial guess for the temperature and moisture profiles used in the inversion, thus being sensitive to the assumed profiles near the surface (Reuter *et al.*, 1988). Typically the IR-retrieved TWP has a wet bias on the order of 10~20% (NASA, 2003e). The TWP amounts that are retrieved from microwave emission measurement, using a similar approach, reveal errors in the order of 10% (Prabhakara

* Corresponding author.
E-mail : spark@ewha.ac.kr, Tel : +82-(0)2-3277-3331

et al., 1982). Furthermore, when the apparent surface temperature is close to the average temperature of the boundary layer, the IR and microwave remote sensing is not sensitive to the boundary layer WV (Gao and Kaufman, 2003; hereafter GK03).

Recently, alternative WV retrieval algorithms have been developed using backscattered near-IR channels around 1 μm (e.g., Thai and Schonermark, 1998; GK03; Bouffies *et al.*, 1997; Kaufman and Gao, 1992 (hereafter KG92)). The MODIS (MODerate-resolution Imaging Spectroradiometer) instruments (NASA, 2003d; King *et al.*, 1992), on board the EOS satellites Terra (NASA, 2003b) and Aqua (NASA, 2003c), have several near-IR channels for measuring radiances from the Earth. In this study, we apply an algorithm (KG92; GK03) to retrieve column WV in the domain of east Asia, using the MODIS near-IR channels, and discuss characteristics of the temporal and spatial distributions of the retrieved fields in the context of potential water resources in that region.

Section 2 briefly introduces the algorithm of retrieving column WV from the MODIS data. Section 3 discusses some retrieval results in both global and east Asia, and section 4 provides conclusions.

Table 1. Positions and bandwidths of five MODIS bands used in water vapor retrievals (both in μm).

Band	Position	Bandwidth
2	0.865	0.841~0.876
5	1.240	1.230~1.250
17	0.905	0.890~0.920
18	0.936	0.931~0.941
19	0.940	0.915~0.965

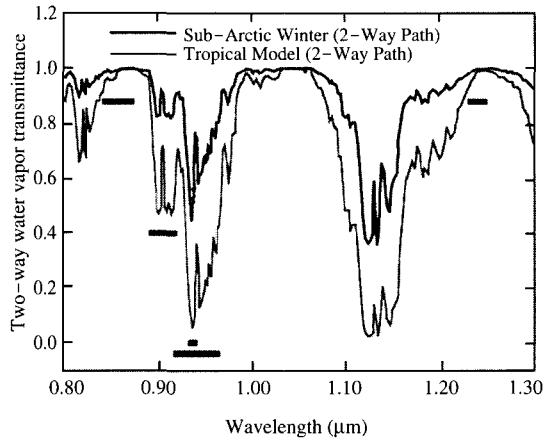

Fig. 1. Positions and bandwidths of five MODIS bands used in water vapor retrievals, marked in thick horizontal bars, along with two-way atmospheric water vapor transmittance spectra for the tropical and subarctic winter models (Kneizys *et al.*, 1988) with a solar zenith angle of 45° and a nadir-looking geometry. From Gao *et al.* (2003) (modified for clarity).

2. ALGORITHM DESCRIPTION

The MODIS measures radiances from the Earth through 36 discrete spectral bands ranging 0.4~15 μm (NASA, 2003d). Spatial resolutions are 0.25 km for bands 1 and 2, 0.5 km for bands 3~7, and 1 km for bands 8~36. Among them, the near-IR channels, especially bands centered at 0.865, 0.905, 0.936, 0.940, and 1.240 μm (see Table 1), are very useful for computing TPW (i.e., column WV) amounts over clear lands, and above clouds over both land and ocean (KG92; GK03).

Among the five near-IR channels, 0.865 μm (band 2) and 1.240 μm (band 5) are WV non-absorption channels which are originally used for remote sensing of vegetation and clouds, while 0.936, 0.940, and 0.905 μm (bands 17~19) are WV absorption channels (see Fig. 1). The total amount of column WV can be derived from a comparison between the reflected solar radiation in the absorption channel and that in nearby non-absorption channels (KG92; GK03).

Retrieval of WV is based on a ratio of absorbing to non-absorbing channels, e.g., a ratio of the measured radiation at 0.940 μm to that of 0.865 μm. The radiance detected at the remote sensor, L_s, is given by

$$L_s = L_t \tau_\lambda r_\lambda + L_p \quad (1)$$

where L_t is the radiance of the targeted area at the top of the atmosphere, τ_λ is transmittance, and r_λ is reflectance. L_p is composed of radiant energy from diffuse

sky irradiance and reflection from nearby areas. Here, τ_λ contains information about total WV amount, and L_p contains WV absorption feature.

The algorithm basically exploits the fact that atmospheric WV has very different absorption coefficients over the bandpasses of MODIS channels centered near 0.905, 0.936, and 0.940 μm. Assuming that surface reflectances are constant with wavelength, the WV transmittance (τ_λ) of the absorbing channel can be obtained through a two-channel ratio of an absorbing channel to a window (nonobsorbing) channel (GK03); for example, the transmittance of the channel at 0.940 μm is

$$\tau_{0.940\,\mu m} = \frac{r^*_{0.940\,\mu m}}{r^*_{0.865\,\mu m}} \tag{2}$$

where r^* is the computed apparent reflectance at the top of the atmosphere for the specified channel, defined as L_s/L_t. When surface reflectances show linear variation with wavelength, a three-channel ratio of an absorbing channel to two window channel is applied; for the same example as above, the three-channel ratio results in

$$\tau_{0.940\,\mu m} = \frac{r^*_{0.940\,\mu m}}{\alpha_1 r^*_{0.865\,\mu m} + \alpha_2 r^*_{1.240\,\mu m}} \tag{3}$$

where α_1 and α_2 are constants. GK03 set the values of α_1 and α_2 to 0.8 and 0.2, respectively.

KG92 showed that, when plotted for the TPW amount using the two-channel ratio, $\tau_{0.905\,\mu m}$ lies below $\tau_{0.940\,\mu m}$ and above $\tau_{0.936\,\mu m}$ for 7 vegetation covers, 15 soil covers, and 2 snow covers. Thus, the 0.940 μm channel is chosen as an optimal channel for retrieving WV in the presence of several centimeters of WV. For low WV content, e.g., much less than 1 cm, the narrow strong-absorbing channel centered at 0.936 μm is more sensitive (KG92), thus making this channel feasible to be used in dry condition. Meanwhile, for WV amount much larger than 4 cm, the strong-absorbing 0.936 μm channel can partially saturate, resulting in low sensitivity to WV; thus the less-absorbing 0.905 μm channel is preferred under humid conditions.

The 2-channel ratio technique is used for WV retrieval over oceanic areas with sun glint while the 3-channel ratio technique is used over clear land (GK03). Since the relationship between τ_λ and TPW (P) is exponential (see Fig. 4 in KG92), τ_λ is related to TPW along the optical path, P^*_λ, as

$$\tau_\lambda = \exp\left(\alpha - \beta\sqrt{P^*_\lambda}\right) \tag{4}$$

where $\alpha = 0.020$ and $\beta = 0.651$ for a mixture of all surfaces (KG92). Then P^*_λ is converted to TPW, P_λ, depending on the solar and the observational geometries as

$$P_\lambda = P^*_\lambda \left(\frac{1}{\cos\theta_v} + \frac{1}{\cos\theta_s}\right)^{-1} \tag{5}$$

where θ_v is the view zenith angle and θ_s is the solar zenith angle. The mean WV value ($\overline{P}$) is obtained according to

$$\overline{P} = w_1 P_1 + w_2 P_2 + w_3 P_3 \tag{6}$$

where P_1, P_2 and P_3 are WVs derived from the three absorbing channels and w_1, w_2 and w_3 are the corresponding weight functions. Detailed description on the algorithm is provided in KG92 and GK03.

As described in previous studies (e.g., KG92; Bouffies *et al.*, 1997; GK03), there exist several sources of errors in the retrieved WV including uncertainties in the sensor calibrations, the spectral reflectance of the surface, pixel registration among several spectral channels, atmospheric profiles of temperature and moisture, and the amount of haze. Errors are also affected by a shift in the channel location, and mixed pixels and clouds (KG92). Among those error sources, it is found that the largest sources of errors are the uncertainty in spectral reflectances of surface targets and the uncertainty in the amount of haze for dark surfaces (KG92; GK03).

Through the regression analysis between the MODIS near-IR WV values and those measured with the ground-based microwave radiometer, GK03 demonstrated that the two data sets are generally in good agreement with a slope of 0.93~0.97 and small offset (0.10~0.06 cm) in the regression line. Typically the

differences between the two data sets are in the range between 5 and 10% (GK03).

In application to spectral data collected by the Airborne Visible Infrared Imaging Spectrometer (AVIRIS), KG92 compared three retrieval methods (curve fitting, 2-channel ratio, and 3-channel ratio) to two ground truth measurements (radiosonde and microwave radiometer) in three different locations. Based on their results, the curve fitting estimate showed almost perfect match with the radiosonde observations while the 3-channel ratio estimate did so with the microwave radiometer (KG92). The former underestimated the microwave radiometer observation by 0.05 cm in average while the latter underestimated the radiosonde observation by 0.11 cm. The 2-channel ratio technique underestimated the WV amount from the ground truth by 0.14 cm in average.

3. ANALYSES OF TOTAL PRECIPITATION WATER

Based on the algorithm described above, the total precipitation water (TPW) fields are analyzed in the global and east Asian atmosphere.

Figure 2 depicts monthly-mean total precipitable water (TPW) in October 2000 and January 2001 from the MODIS product (MOD05). It is noted that subtropical maximum of TPW in the fall is observed in southeastern Asia at around $10°S-30°N$ and in South America over $15°S-15°N$. The global amount of TPW decreases significantly in the northern hemisphere during winter, showing remarkable seasonal variation, especially in the northern hemisphere. Only moderately-high amount of TPW is observed in southern hemispheric South America and in a narrow band in eastern Asia near the equator. It is evident that long-term analyses of the global TPW would allow us to examine sources and sinks of the global water as well as trend in the regional water amount.

Figure 3 shows monthly-mean TPW for October 2000 in the Asian region. Southern Asia still holds a great amount of TPW with the largest amount being confined to the regions of lower latitude (below $30°N$). A big contrast is eminent in northern Asia and Siberia with the smallest amount of TPW (dry) over Tibetan Plateau and Siberia. In particular, a sharp gradient in TPW occurs just south of Tibetan Plateau. An interesting feature is a relatively high amount of TPW that is recognized over the central part of Tibetan Plateau. This seems to be strongly related to the high-level clouds observed in that area (see Gao *et al.*, 2003).

The MODIS scans almost the same area of the Earth with an eight-days interval. Thus, it is meaningful to examine the eight-days mean in TPW. Figure 4 shows eight-days mean TPW from October 7, 2000. A significant decrease in TPW is observed as time approaches the end of October, as illustrated by the decrease of the areas where the TPW amounts are over 6 cm (areas with black squares). The boundary of sharp contrast also retreats to the south with time. It is also notable that the central part of Tibetan Plateau clearly has relatively larger amount of TPW than surrounding areas. This kind of analysis is very useful to examine the short-time variation in TPW, especially at local regions. Near-weekly forecast of TPW may also be possible through detailed trend analysis.

4. CONCLUSIONS

In this study, total precipitable water (TPW) in both global and regional scale has been retrieved from the near-infrared spectral bands in MODIS, which is on-board the EOS flagship Terra satellite.

The retrieval algorithm is based on the ratio technique between the water vapor absorption and atmospheric window channels, as depicted in KG92 and GK03. Based on this algorithm, distributions of the TPW fields are discussed over the global and east Asian domain for the seasons of fall and winter. Tropical and subtropical areas of southeastern Asia as well as South America show the largest amount of TPW in the global atmosphere, whereas the seasonal

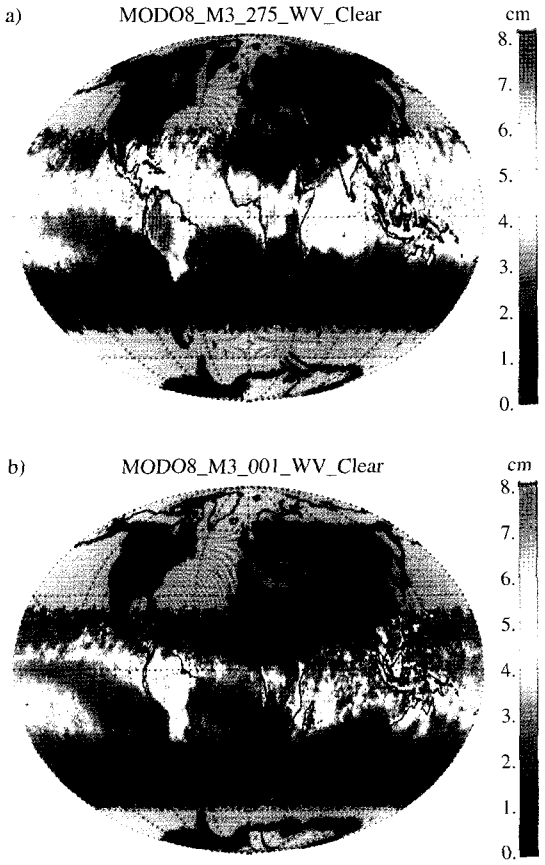

Fig. 2. Monthly-mean total precipitable water for a) October 2000 and b) January 2001 (in cm).

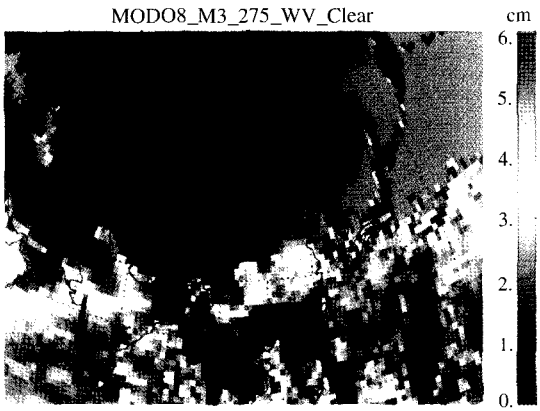

Fig. 3. Monthly-mean total precipitable water in the Asian region for October 2000. Black squares indicate areas of TPW larger than 6 cm.

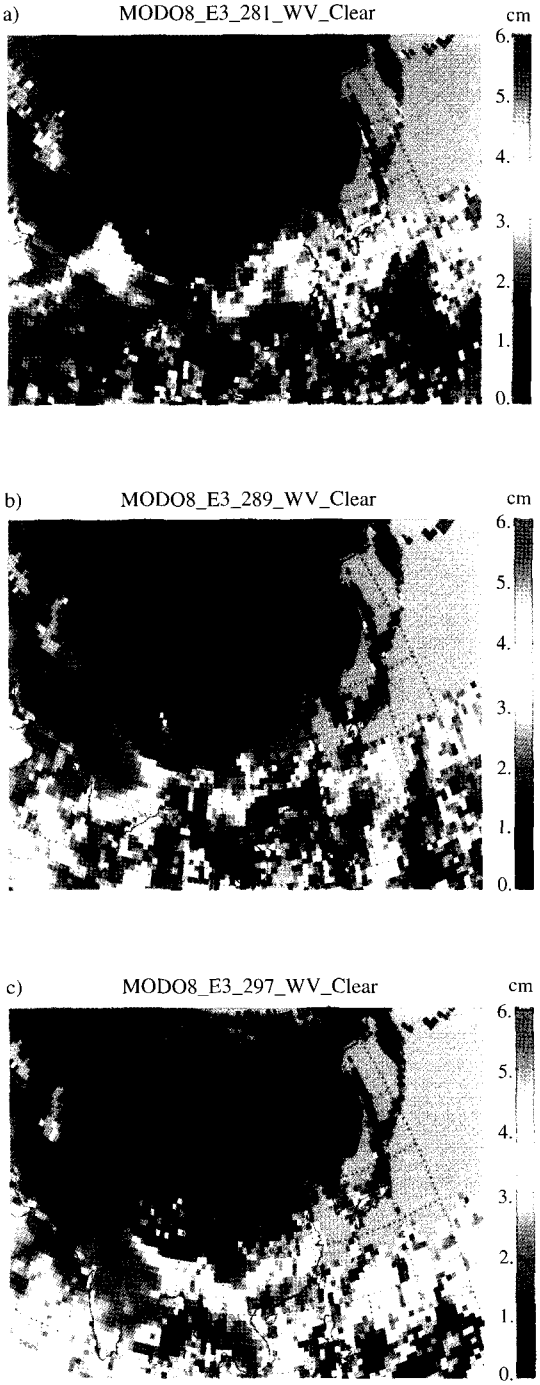

Fig. 4. Same as in Fig. 3 except for the eight-days mean total precipitable water for the period of a) October 7~14, b) October 15~22, c) October 23~30 in the year of 2000.

variation from fall to winter is significant. A sharp contrast in the amount of TPW is eminent between northern Asia (including Tibet and Siberia) and southern Asia. As such, the global and regional analyses of monthly-mean TPW allow us to monitor the characteristics of amount and distribution (i.e., water resources), and seasonal variations in TPW at both global and local regions.

Through an eight-days analysis of TPW, a near-weekly variation in local regions is available and thus short-term forecast of water resources is possible when correct trend analysis is provided. A long-term monitoring will be essential to understand the characteristics of global and regional variations in water resources through the TPW analysis. In particular, monitoring of TPW through remote sensing technique is extremely useful to compensate the sparse ground monitoring stations, especially in drought regions, to provide accurate water resource information with a high spatial resolution (e.g., 1~5 km from MODIS). The MODIS instrument is also on-board Aqua (formerly EOS-PM; NASA 2003d) satellite, the second EOS flagship, which was launched in May 2002. Therefore, continuous monitoring of TPW will be available for at least next 7 years.

ACKNOWLEDGMENTS

The author is grateful to Dr. B.-C. Gao at Naval Research Laboratory for providing the analysis code. Part of this research was conducted while the author was in the US NASA/Goddard Space Flight Center. The author also acknowledges Prof. P. Yang at Texas A & M University for his help in this research. This research is supported by the Intramural Research Grant by the Ewha Womans University.

REFERENCES

Barron, E.J., D.L. Hartmann, M.D. King, D.S. Schimel, and M.R. Schoeberl (1999) Overview, In *EOS Science Plan-The State of Science in the EOS Program*, NP-1988-12-069-GSFC, NASA/GSFC, 387 pp.

Bouffies, S., F.M. Breon, D. Tanre, and P. Dubuisson (1997) Atmospheric water vapor estimate by a differential absorption technique with the polarization and directionality of the Earth reflectances (POLDER) instrument, J. Geophys. Res., 102, 3831-3841.

Chesters, D., L.W. Uccellini, and W.D. Robinson (1983) Low level water vapor fields from the VISSR atmospheric sounder (VAS) split window channels, J. Climate Appl. Meteor., 22, 725-743.

Gao, B.-C. and Y.J. Kaufman (2003) Water vapor retrievals using Moderate Resolution Imaging SPectroradiometer (MODIS) near-infrared channels, J. Geophys. Res., 108(D13), 4389-4398.

Gao, B.-C., P. Yang, G. Guo, S.K. Park, W.J. Wiscombe, and B. Chen (2003) Measurements of water vapor and high clouds over the Tibetan plateau with the Terra MODIS instrument, IEEE Trans. Geosci. Remote Sensing, 41, 895-900.

Kaufman, Y.J. and B.-C. Gao (1992) Remote sensing of water vapor in the near IR from EOS/MODIS, IEEE Trans. on Geosci. Remote Sensing, 30, 871-884.

King, M.D., Y.J. Kaufman, W.P. Menzel, and D. Tanre (1992) Remote sensing of cloud, aerosol, and water vapor properties from the Moderate Resolution Imaging Spectrometer (MODIS), IEEE Trans. Geosci. Remote Sensing, 30, 1-27.

Kleespies, T.J. and L.M. McMillin (1990) Retrieval of precipitable water from observations in the split window over varying surface temperatures, J. Appl. Meteor., 29, 851-862.

Kneizys, F.X., E.P. Shettle, L.W. Abreu, J.H. Chetwynd, G.P. Anderson, W.O. Gallery, J.E.A. Selby, and S.A. Clough, Users Guide to LOWTRAN 7, AFGL-TR-8-0177, Air Force Geophys. Lab., Bedford, Mass., 1988.

NASA, cited 2003a: EOS: Earth Observing System, Available online from "http://eos.gsfc. nasa.gov/".

NASA, cited 2003b: TERRA: The EOS Flagship, Available online from "http://eos-am.gsfc.nasa.gov/".

NASA, cited 2003c: Aqua Website, Available online from "http://aqua. gsfc.nasa. gov/".

NASA, cited 2003d: MODIS Web, Available online from "http://modis.gsfc. nasa.gov/".

NASA, cited 2003e: MODIS Atmosphere, Available online from "http://modis-atmos.gsfc. nasa.gov/".

Prabhakara, C., H.D. Chang, and A.T.C. Chang (1982) Re-

mote sensing of precipitable water over the oceans from Nimbus 7 microwave measurements, J. Appl. Meteor., 31, 59-68.

Reuter, D., J. Susskind, and A. Pursch (1988) First-guess dependence of a physically based set of temperature-humidity retrievals from HIRS2/MSU data, J. Atmos. Ocean. Tech., 5, 70-83.

Thai, S. and M.V. Schonermark (1998) Determination of the column water vapor of the atmosphere using back-scattered solar radiation measured by the Modular Optoelectronic Scanner (MOS), Int. J. Remote Sens., 19, 3223-3236.